NASA CONTRACTOR REPORT

NASA CR-

NASA CR-2666

VACUUM ULTRAVIOLET SPECTRA OF URANIUM HEXAFLUORIDE/ARGON MIXTURES

N. L. Krascella

Prepared by
UNITED TECHNOLOGIES RESEARCH CENTER
East Hartford, Conn. 06108
for Langley Research Center

NATIONAL AERONAUTICS AND SPACE ADMINISTRATION • WASHINGTON, D. C. • MARCH 1976

1. Report No.	2. Government Accession No.	3. Rec
NASA CR-2666		

4. Title and Subtitle	5. Report Date
VACUUM ULTRAVIOLET SPECTRA OF URANIUM HEXAFLUORIDE/ ARGON MIXTURES	MARCH 1976
	6. Performing Organization Code
7. Author(s)	8. Performing Organization Report No.
N. L. Krascella	
	10. Work Unit No.
9. Performing Organization Name and Address	
United Technologies Research Center East Hartford, Conn. 06108	11. Contract or Grant No. NAS 1 13291
	13. Type of Report and Period Covered Contractor Report
12. Sponsoring Agency Name and Address	
National Aeronautics and Space Administration Washington, DC 20546	14. Sponsoring Agency Code

15. Supplementary Notes

Project Manager, Frank Hohl, Environmental and Space Sciences Division, NASA, Langley Research Center, Hampton, VA

TOPICAL REPORT

16. Abstract

The transmission properties of room temperature helium at pressures up to 20 atmospheres were determined in the wavelength range from 80 to 300 nm. Similarly, the transmission properties of uranium hexafluoride at 393 K (pressures less than 1.0 mm) were determined in the wavelength range from 80 to about 120 nm.

The results show that high-pressure helium is sufficiently transparent in the vacuum ultraviolet region (provided trace contaminants are removed) to be utilized as a transparent purge gas in future fissioning gaseous uranium plasma reactor experiments. Absorption cross sections for uranium hexafluoride were calculated from the data between 80 and 120 nm and were of the order of 10^{-17} cm^2.

17. Key Words (Suggested by Author(s)) (STAR category underlined)	18. Distribution Statement
Gas-Core Reactor VUV Spectroscopy High Pressure Optical Path Ar/UF_6 Spectral Absorption	Unclassified - Unlimited Subject Category 73

19. Security Classif. (of this report)	20. Security Classif. (of this page)	21. No. of Pages	22. Price*
Unclassified	Unclassified	39	$3.75

CONTENTS

VACUUM ULTRAVIOLET SPECTRA OF URANIUM HEXAFLUORIDE/ARGON MIXTURES

N. L. Krascella

United Technologies Research Center

SUMMARY

This study was initiated to provide basic data with respect to the attenuation of vacuum ultraviolet (VUV) radiation by helium at pressures up to 20 atm over path lengths of about 61 cm and in the approximate wavelength range between 80 and 300 nm. These data are required to assess the possible utilization of helium as a transparent purge gas in the optical path through the reflector-moderator of an experimental, high pressure, fissioning gaseous uranium hexafluoride (UF_6) reactor and a vacuum ultraviolet spectrometer. The spectral measurements in the reactor experiment would be undertaken to determine the VUV emission characteristics of fissioning UF_6 gas and uranium plasmas and to determine the extent of nonequilibrium emission due to deposition of fission fragment energy in the gaseous nuclear fuel.

Similarly, measurements were conducted to provide basic VUV spectral data (currently unavailable in the literature) with respect to UF_6 and UF_6/argon mixtures in the wavelength range between 80 and 120 nm. These data are required for theoretical analysis of radiatien transport in the buffer gas region of a plasma core reactor. These results would also provide baseline data for subsequent investigation of fission-fragment induced nonequilibrium radiation effects in the VUV spectral region in future planned gaseous UF_6 cavity reactor experiments.

Transmission measurements were made in helium contained in a 61-cm-long cell in the wavelength range between 60 and 300 nm. Gas pressures were varied from a few tenths of an atmosphere to about 20 atm. Spectral data were obtained for standard tank gas as received and over limited spectral regions for helium which was partially purified by passing through a liquid-nitrogen cooled zeolite trap. The trap served to remove trace quantities of impurities normally found in helium. Similar measurements were made in argon at a wavelength range between 80 and 120 nm to provide baseline data for subsequent measurements in UF_6/argon mixtures. The argon tests were conducted in a 61 cm cell at pressures up to approximately 3 atm. No attempts were made to remove trace contaminants from the argon.

Finally, the transmission properties of UF_6 diluted with argon were measured in a 1.91-cm-long cell over a range of UF_6/argon partial pressure ratios from 7×10^{-3} to 5.5×10^{-2} and in the wavelength range between 80 and 200 nm. Subsequently, the transmission results were used to determine the spectral absorption cross sections of UF_6 over the wavelength range between 80 and 120 nm.

SYMBOLS

I	transmitted intensity, arbitrary units
I_o, I_o'	incident or source intensity, arbitrary units
L	path length, cm
ln	natural logarithm
N	number density, cm^{-3}
P	pressure, atm or mm Hg
Q	volumetric flow rate, liter/min at standard conditions
T	temperature, deg K
T'	transmission $(I/I_o \times 100)$ or $(I/I_o' \times 100)$
λ	wavelength, nm
σ	absorption cross section, cm^2

INTRODUCTION

Extensive experimental and theoretical research has been conducted with respect to various aspects of fissioning gaseous plasmas over the past two decades. These studies have been generally directed toward high performance nuclear space propulsion systems (ref. 1). In addition to space applications, the Plasma Core Reactor (PCR) concept has been recognized as a possible candidate energy source for various terrestrial applications (ref. 2). The very high operating temperatures generated by fissioning plasmas tend to enhance efficiencies of various thermodynamic cycles compared to conventional power generating systems or nuclear reactors with solid fuel elements. Furthermore, the high operating temperatures associated with gaseous fissioning reactors provide a source of very intense electromagnetic radiation with a number of possible applications involving direct coupling of energy by radiative processes.

Although most of the applications of the PCR require extensive basic research and technological development, the potential benefits from the use of these devices warrant continued investigation of the concept. Possible PCR space and/or terrestrial applications are:

(1) High-thrust, high-specific-impulse space propulsion systems.

(2) Advanced high-temperature, closed-cycle gas turbine electrical power generation.

(3) MHD conversion systems for electrical power generation.

(4) Photochemical and/or thermochemical processing.

(5) Direct pumping of lasers by deposition of fission fragment energy in UF_6 or other lasing gas mixtures.

(6) Optical pumping of lasers by thermal and/or nonequilibrium radiation emitted by a gaseous fissioning UF_6 or uranium plasma.

A typical unit cell of a PCR device is illustrated in figure 1. In the PCR concept a high-temperature, high-pressure plasma is sustained via the fission process in a uranium gas injected as UF_6 or other uranium compounds. Containment of the plasma is accomplished fluid-mechanically be means of an argon-driven vortex which also serves to thermally isolate the hot fissioning gases from the surrounding wall.

For applications which employ thermal radiation emitted from the plasma, an internally-cooled transparent wall can be employed to isolate the nuclear fuel, fission fragments, and argon in a closed-circuit flow loop and permit transfer of the radiant energy from the plasma to an external working fluid. For applications which employ fission fragment induced short wavelength non-equilibrium radiation emitted from the plasma, the working fluid such as lasing gases can be either mixed with fissioning gas or injected into the peripheral buffer gas region such that there is no blockage of radiation due to the intrinsic absorption characteristics of transparent materials at short wavelengths.

Three fundamental areas of research are required to demonstrate the feasibility of the PCR concept: (1) nuclear criticality; (2) fluid mechanical confinement; and, (3) transfer of energy by radiation processes. Various aspects of these areas of technology are currently being investigated at United Technologies Research Center (UTRC). In addition, cavity reactor experiments which will employ gaseous UF_6 are currently being performed at Los Alamos Scientific Laboratory (LASL) as part of the planned NASA program to determine the feasibility of plasma core reactors.

The present paper summarizes results of transmission measurements in various gases of interest to PCR technology. These data were required to assess the use of high pressure helium as a transparent purge gas in future VUV radiation studies of fission-fragment-induced nonequilibrium radiation emitted from fissioning uranium gases in cavity reactor experiments. In addition, transmission measurements in various UF_6/argon mixtures were undertaken to provide spectral data in the VUV required for subsequent radiative transfer analyses.

TEST EQUIPMENT

A McPherson Model 235, half-meter scanning monochromator was used for all spectral measurements. A schematic diagram of the monochromator and accessories, gas cell and gas handling system, is shown in figure 2 and is photographically displayed in figure 3. The monochromator was of the Seya-Namioka type and had a full aperture ratio of f/11.4. Wavelength scan rates were variable in twelve steps from 0.025 nm/min to 100 nm/min. A 10.2 cm, 750 liter/s high-speed, oil-diffusion pump and a 425 liter/min Welch mechanical pump comprised the basic pumping system for the monochromator. The monochromator was equipped with a 1200 line/mm grating, blazed at 150 nm· which allowed measurements in the wavelength range between 50 and 300 nm. The linear dispersion of the grating was quoted to be 1.66 nm/mm. Resolution was 0.05 nm when used with 10 μ slits.

Model 820 differential slits systems were used at both the entrance and exit ports of the monochromator. Each differential slit system was equipped with slits of widths of 10, 50, and 100μ.

A McPherson Model 630 high energy, VUV, Hinteregger-type discharge lamp was used as the source of radiation in conjunction with a Model 720 high-voltage dual-mode power supply. The source system can be operated as an air-gap controlled, high-voltage spark or as an ac arc. Only the former operating mode was used during the study since the spark mode provided enhanced continuum radiation when the lamp was charged with various rare gases. Helium, argon, and xenon were used as source gases and provided continuum radiation in the approximate wavelength range between 60 and 200 nm. The approximate useful wavelength ranges for these rare gases were:

Gas	Range-nm
Helium	60.0 - 105.0
Argon	105.0 - 145.0
Xenon	145.0 - 195.0

A simple Westinghouse tungsten-iodine lamp was used as the radiation source in the wavelength range between 200 and 300 nm.

The radiation detector system consisted of a McPherson Model 650 detector assembly and a Model 790 detector electronic system. The detector contains a sodium salicylate coated window and a Model 9514B phototube. Ultraviolet radiation incident upon the sodium salicylate causes fluorescence at about 400 nm which is subsequently detected by the photomultiplier, amplified, and recorded. Although the sodium salicylate/photomultiplier system is sensitive from 50 to 600 nm, the linear response range was from 50 to about 300 nm.

Two gas cells were designed and fabricated for the transmission measurements. Transmission measurements in high pressure helium were made in a 7.6-cm-ID,61-cm-long stainless steel cell as shown in figure 2. The cell was positioned between the monochromator exit slit and the detector. Pressure transducers and thermocouples were connected to the test cell to permit pressure and temperature monitoring. Since the pumping speed is greatly attenuated through small slits, a separate mechanical vacuum pump was used to assist in evacuating the test cell as shown in figure 2.

Although initial experiments with UF_6/argon mixtures were attempted in the 61 cm cell, the mixtures proved to be extremely opaque and no radiation was transmitted through the 61 cm path length. A short-path-length cell was constructed of 5-cm-dia copper tubing in which the spectral transmission properties of various UF_6/argon mixtures were determined (see fig. 4). The length of this cell was 1.91 cm. A 0.95-cm-OD inlet port with provision for a thermocouple and a 0.95-cm-OD outlet port with provision for a pressure transducer were located at the axial midpoint. The copper cylinder was soldered to two 10.2-cm-dia brass flanges which provided mounting to the exit slit and subsequent mounting of the detector housing. Initially, 1.9-cm-dia ports in each flange permitted passage of radiation through gas samples. Each flange was drilled with two inlet and exit (0.32 cm) injectors through the 0.95 cm thickness to permit injection of argon at one side of the optical aperture. Ports opposite the argon injectors were installed to allow pumping of injected argon in an attempt to prevent flow of UF_6 into the monochromator chamber and to prevent deposition or reaction of UF_6 on or with the sodium salicylate. Since the system provided marginal protection to the sodium salicylate coating, subsequent experiments were performed with one argon inlet port at the entrance to the cell and with all four ports at the cell exit also injecting argon into the cell. In addition, an insert was machined to reduce the area of sodium salicylate exposed to UF_6 and placed in the cell exit flange. An aperture located in the insert 0.48 cm in width and 1.59 cm in height allowed the radiation to pass through gases in the cell. In this configuration, all argon injected into the cell was pumped out through the UF_6/argon exit port located at the axial midplane of the cell proper. With this flow arrangement, no degradation of the sodium salicylate coating was observed. Similarly, no evidence of condensation of UF_6 on the monochromator exit slit system or on the grating was evident by physical inspection or by spectral monitoring before or after exposure to UF_6.

The UF_6 handling system consisted of a stainless steel UF_6 supply cylinder, a sodium fluoride (NaF) trap, and appropriate shutoff and metering valves. The NaF trap was installed to remove traces of HF usually found admixed with UF_6. Six thermocouples were installed to monitor temperatures at various strategic locations. These details are shown in figure 2. Argon was supplied to the system via the cell injectors previously described. All lines, the test cell, and associated equipment were electrically-heated by means of controlled heater tapes.

A zero-to-50 mm Hg Wallace and Tiernan absolute pressure gauge was used to monitor monochromator chamber pressures. Similarly, a 0-to-200 mm Hg Wallace and Tiernan absolute pressure gauge was used to monitor source-lamp gas pressures. Absolute pressure transducers of appropriate ranges were mounted on the test cells to ascertain gas pressures in the gas cells. Pressure transducer output was displayed on a recorder as well as on a vacuum tube volt meter.

The helium and argon used for the VUV lamps and the various test gases could be passed through zeolite traps cooled with liquid nitrogen or an alcohol/dry ice mixture. Cooled traps were absolutely necessary to remove trace impurities from these gases when used in the VUV lamp. Although high purity helium and argon were used (99.9999% helium or argon), no continuum was observed without prior removal of trace impurities.

Spectrometer Modifications

One objective of the current investigation involved the study of the transmission characteristics of helium over long path lengths and at high pressures up to approximately 20 atm. As implied by nomenclature, a VUV spectrometer is normally operated under vacuum conditions or at least under reduced pressures. Consequently, these instruments are designed to seal under reduced pressures but not if internal pressures exceed atmospheric pressure. Therefore, a number of modifications were required (1) to enable sealing of the sodium salicylate window under either vacuum or high pressure operating conditions, and (2) to prevent distortion of the thin metal plates forming the exit slit of the differential slit assembly. The detector flange supplied with the Model 630 detector assembly was replaced with an alternative flange system as shown in figure 5 which allowed changes in pressures from about 5×10^{-6}-mm-Hg to 20 atm without apparent leakage of gases or expulsion of the sodium salicylate holder against the photomultiplier tube. Similarly, two stainless steel inserts were machined and installed between the three 0.16 cm plates delineating the two differential slit assembly pumping chambers (see fig. 6). These inserts contained ports at four positions to allow individual pumping of each chamber as originally designed and if required. The modified exit slit assembly was successfully operated at pressures approaching 20 atm without apparent distortion or damage.

Differential Slit Pressure and Flow Tests

A series of pressure and flow tests was conducted using the modified differential slit assembly to verify integrity of the optical slit system at pressures up to 20 atm. These tests also provide data with regard to pressure drops across the slit system and flow data for helium under high pressures. A schematic of the experimental layout used for these tests is shown in figure 7. A Fischer-Porter flow meter was used to monitor flow and was subsequently calibrated against a Matheson linear mass flow meter of known precision. Pressures in various chambers were monitored by means of pressure transducers in each chamber. Helium was used as the test gas during these studies and was exhausted to atmospheric pressure. Volumetric flow results

obtained during these tests are shown in figure 8 as a function of upstream pressure (simulated test cell gas pressure). These results indicated that only the 10 μ slit would be usable for subsequent spectral studies in helium at pressures up to 20 atm. For example, a standard 1A cylinder of helium contains 6940 liters of gas at standard conditions. Extrapolating the volumetric flow data (fig. 8) to 20 atm (for a 50 μ slit) indicates that a cylinder of helium would be expended in approximately 15 minutes. Thus, subsequent spectroscopic data were obtained using only the 10 μ exit slit to permit long-duration tests.

Pressure data for various differential slit chambers, as well as simulated monochromator and test cell chambers, indicated that in each test all the pressure reduction occurred across the variable slit S_1. Negligible or no pressure drops occurred across slits S_2 and S_3 which were at fixed dimensions.

EXPERIMENTAL PROCEDURES AND OPERATING PARAMETERS

All spectral measurements from approximately 60 to 300 nm were conducted in a windowless mode. No differential pumping was used for any of the tests conducted. A 2123 liter/min auxiliary pump was used on the first chamber of the differential exit slit system to assist the spectrometer mechanical pump during actual measurements. With this arrangement, monochromator chamber pressure was always less than about 25-mm-Hg. Helium and argon transmission measurements were made using the 61-cm-long test cell between the monochromator exit slit and the detector. A 1.91-cm-long cell was used for the UF_6 tests.

Standard quality helium and argon (99.995% rare gas) were used for the test gas except where noted. A pressure transducer of the appropriate range was used to monitor test gas pressures during various tests. Pressure transducer output was monitored on one channel of a two-channel recorder. The second recorder channel was used to monitor spectrometer detector output. Because of occasional rf interference from adjacent experiments in the laboratory, the pressure transducer output was also monitored on a Hewlett-Packard vacuum tube multirange volt meter. The rf interference caused erratic behavior of the recorder pressure transducer trace. A copper-constatan thermocouple was used to monitor gas temperatures in the test cell. For helium and argon measurements, temperature was a constant 298 K for all tests. For the UF_6/argon tests, temperature was constant at 393 K, as monitored in the test cell and at various points in the gas handling-transfer system.

High-purity helium and argon (99.9999% rare gas) used as source-lamp gases required removal of trace impurities to allow significant intensity of their respective continua. The trap material was zeolite cooled with liquid nitrogen when helium was used and alchohol/dry ice mixture when argon was used. A trap was not required or used with xenon as the source gas. Gas pressures for the VUV sources were usually of the order of 50 to 120-mm-Hg. No attempt was made to optimize the continuum emitted by the VUV lamp other than setting lamp pressure to maximize continuum output while minimizing the height of lines superimposed on the continuum.

In most cases, the spectrometer entrance slit was fixed at 50μ and the exit slit at 10μ. With these slit settings, the detector voltage and amplification and recorder gain were set to provide maximum recorder deflection with minimum noise.

Helium and argon spectra were scanned at 10 nm/min while the rate of scanning for UF_6 spectra was 25 nm/min. The higher scan rate for the UF_6 measurement was selected to minimize exposure of the equipment to UF_6 vapor.

Normal procedure included at least two I_o determinations in the evacuated system to insure stable operating conditions. Both lamp and monochromator pressure were monitored during these tests. For the rare gas transmission tests, the cell was filled to the required pressure and the flow allowed to equilibrate prior to conducting a wavelength scan. VUV lamp pressure, monochromator pressure, and cell pressure were recorded during the spectral scans. After a series of transmission measurements, usually one or two, the test cell was evacuated and either I_o redetermined or a selected wavelength (wavelength at the continuum peak) monitored to insure no changes had occurred during the preceding tests. I_o tests were made with both the diffusion pump and 425 liter/min mechanical pump operating. Wavelength scans with the test gas were made with the 425 liter/min and 2123 liter/min mechanical pumps operating.

A similar procedure was followed for the UF_6 measurements. Initial I_o was determined in the evacuated system followed by an I_o' determination in which argon was allowed to flow in the test cell at a fixed pressure (no UF_6 flow). Subsequently, UF_6 was introduced into the cell, the pressure increase noted, and the wavelength scans with UF_6/argon were conducted. Upon completion of the spectral scan with UF_6/argon mixture, the UF_6 flow was terminated and the cell was pumped for approximately 15 to 20 minutes to evacuate UF_6. As in previous tests with the rare gases, I_o' was redetermined or, for convenience, a particular peak in the previous I_o' scan was monitored to insure constancy of conditions between scans. This procedure also served to establish that UF_6 contamination of the sodium salicylate had not

occurred. After two or three tests with UF_6, the sodium salicylate window was removed for visual inspection of UF_6 contamination. The sodium salicylate was routinely replaced at these times.

SPECTRAL RESULTS AND DISCUSSION OF RESULTS

Helium

A series of experiments was conducted in the apparatus previously described to determine the transmission properties of standard helium gas at high pressures. All transmission measurements were made in the 61-cm-long cell at room temperature. The wavelength ranges and helium pressures for which optical data were measured in this series of tests are summarized in Table I. Table I also includes pressure and wavelength ranges for two series of experiments involving helium from which contaminants were partially removed by a cooled zeolite trap and similar data for experiments with standard argon as the test gas.

Recorder traces of the relative spectral intensities determined during the experiments are shown in figures 9 through 12 for standard helium gas in the approximate wavelength range between 60 and 300 nm. Each figure illustrates I_o, the source intensity without test gas in the cell, and intensity scans I_1 and I_2 for two representative pressures of helium in the test cell. Additional experimental parameters (wavelength scan rates, slit settings, etc.) are listed in Table II for each set of spectral measurements.

As the results illustrate, standard tank helium at pressures as low as 3.7 atm is relatively opaque in the VUV at wavelengths between 60 and 110 nm (see fig. 9). At a pressure of 9 atm, the gas is almost totally opaque to VUV radiation. Figure 10 illustrates similar transmission data for standard tank helium between 100 and 160 nm. These results were obtained at 4.7 and 18.7 atm and show that the helium is relatively transparent in this wavelength interval. At a wavelength of about 128 nm, the transmission is approximately 65% at a helium pressure of 18.7 atm. Similar experimental results are shown in figure 11 in the wavelength range between 145 and 200 nm at helium pressures of 8.8 and 17.7 atm. The transmission of helium is of the order of 63% at a pressure of 17.7 atm and at a wavelength of 170 nm. Figure 12 illustrates the transmission properties of helium in the wavelength range between 220 and 300 nm for helium pressures of 5.4 and 18.3 atm. The results indicate that helium is relatively transparent in this wavelength range. For example, the transmission is of the order of 60% at a wavelength of 296 nm at a helium pressure of 18.3 atm.

As indicated by the spectral transmission results over a range of wavelengths and pressures, standard tank helium could be used as a transparent purge gas at high pressure approaching 20 atm in subsequent nuclear reactor tests at wavelengths greater than 100 nm. At wavelengths shorter than 100 nm, the standard tank gas is relatively opaque to radiation even at modest pressures ($\sim$4 atm).

Since the excited state population of room temperature helium is negligible, absorption of radiation in helium should occur only at wavelengths below 50 nm, the threshold for the boundfree continuum from the ground state. The marked attenuation of radiation in the wavelength interval between 60 and 100 nm is undoubtedly due to trace contaminants. These impurities are generally O_2, H_2, N_2, CO_2, and H_2O which constitute about 5×10^{-3} percent of the gas. Theoretical estimates of the transmission of high purity helium (99.9999% helium), based on contaminant absorption coefficient data of reference 3, indicated about 30% transmission in high purity helium at 20 atm and over a path length of 60 cm in the VUV region.

Subsequently, a liquid-nitrogen-cooled zeolite trap was installed in the helium gas supply system to partially remove trace contaminants. A second series of transmission studies was conducted to determine the transmission properties of helium after removal of trace impurities. Spectral data (60 to 110 nm) at helium pressures of 7.3 and 18.5 atm are shown in figure 13. These data indicate that the transmission characteristics of helium are greatly improved if the helium is passed through a liquid nitrogen-cooled, zeolite trap prior to the spectral measurements. Appreciable transmission was observed at helium pressures up to 18.5 atm with "clean" helium (fig. 13) as compared to the untreated helium at 9 atm (fig. 9).

Argon

Similar transmission measurements were made with standard tank argon (99.995%) in the spectral interval between 60 and 110 nm. These data were required to determine the approximate quantities of argon to be used in subsequent UF_6/argon tests and to provide basic transmission data related to the buffer gas region of a PCR. Typical experimental transmission results as a function of wavelength are shown in figure 14 for argon pressures of 0.13 and 0.46 atm. Argon is relatively opaque in this spectral region, as illustrated in figure 14. Since threshold for the first boundfree continuum in argon is at a wavelength of approximately 80 nm and extends to shorter wavelengths, no transmission was expected or observed below 80 nm. As in the case of helium, the marked attenuation of the radiation observed is probably due to trace contaminants. No attempts were made to remove contaminants as in the case of helium.

Uranium Hexafluoride

A series of transmission studies was conducted in mixtures of UF_6 and argon at various partial pressure ratios (P_{UF_6}/P_{Ar}). A summary of the pressures of argon and UF_6 as well as the corresponding partial pressure ratios used are tabulated in Table III. Other experimental parameters are shown in Table II. All measurements were made at a temperature of 393 K and over a path length of 1.91 cm. The wavelength interval extended from 60 nm to approximately 200 nm.

Typical spectral transmission results for UF_6/argon mixtures are shown in figure 15 for the wavelength interval between 60 and 120 nm and in figure 16 for the wavelength interval between 120 and 200 nm. Curve 1 represents the relative source intensity I_o, without gases in the test cell, while curve 2 shows the relative intensity I_o', after introduction of argon into the cell at a pressure of 45.8-mm-Hg. Curves 3 and 4 illustrate the transmission spectra of UF_6/argon mixtures with UF_6 partial pressures of 1.78 and 0.48-mm-Hg, respectively. Similar data were obtained for the other conditions listed in Table III. A partial pressure of less than 2-mm-Hg of UF_6 reduces the transmission by about 85% throughout this spectral region.

The results displayed in figure 15 were used to determine absorption cross sections for UF_6 in the VUV region. The cross section is defined by the relationship:

$$I/I_o' = \exp - \sigma N L \qquad (1)$$

where I is the transmitted intensity, I_o' is the incident intensity; σ the absorption cross section, N the absorber density, and L the path length (1.91 cm). The incident intensity used in these calculations was I_o', the relative intensity with argon in the test cell (fig. 15, curve 2). The quantity I/I_o' was determined at wavelength intervals of 2.5 nm between 80 and 120 nm. These data (I/I_o') are plotted as a function of wavelength in figures 17 and 18 for five partial pressures of UF_6 investigated. Number densities were determined from knowledge of the UF_6 pressure (Table III) and temperature as follows:

$$N = 7.341 \times 10^{21} \frac{P(atm)}{T} \qquad (2)$$

Subsequently, cross section data were calculated for the five sets of experimental data by means of equation (3):

$$\sigma = -(\ln \frac{I}{I_o})/NL \qquad (3)$$

These results are summarized in Table IV. The last column in Table III are the calculated average values of the absorption cross section at various wavelengths. Average cross section results are graphically illustrated in figure 19 as a function of wavelength.

The cross section results shown in Table IV and figure 19 exhibit a range of values from about 6×10^{-18} to 2.7×10^{-17} cm^2. As shown in figure 19, the data below approximately 95 nm, are reasonably smooth with relatively small scatter. At wavelengths greater than 95 nm, determination of the relative intensities with precision is difficult due to the low intensity from the VUV source. Thus, small errors in determining I_o' or I or random noise on the traces result in the scatter observed in the data at wavelengths greater than 95 nm.

CONCLUSIONS

In summary, the transmission characteristics of helium, argon, and UF_6/argon mixtures have been experimentally examined over a range of wavelengths and pressures. The helium results indicate that helium could be used as a high pressure, transparent purge gas in future fissioning plasma VUV emission studies provided trace impurities are sufficiently removed. In addition, the cross section results obtained for UF_6 in the VUV region represent the only known quantitative data available for this compound. These cross section data will be used in subsequent analytical radiation transport analyses related to performance studies of the PCR concept and experiments.

REFERENCES

1. Thom, K., R. T. Schneider, and F. C. Schwenk: Physics and Potentials of Fissioning Plasmas for Space Power and Propulsion. Paper No. 74-087. Int'l. Astronautical Federation (IAF) XXVth Cong., Amsterdam, 30 Sept. - 5 Oct. 1974.

2. Latham, T. S., F. R. Biancardi, and R. J. Rodgers: Applications of Plasma Core Reactors to Terrestrial Energy Systems. AIAA Paper 74-1074, AIAA/SAE 10th Propulsion Conference, San Diego, Calif., Oct. 21-23, 1974.

3. Allen, L.: Astrophysics. Ronald Press, New York, 1953.

TABLE I

PRESSURES AND WAVELENGTH RANGES FOR RARE GAS MEASUREMENTS

Gas	Wavelength Range (nm)	Pressure (atm)	Gas	Wavelength Range (nm)	Pressure (atm)
Helium (99.995%)	60-110	0.20	Helium (99.995%)	220-300	1.21
		0.45			5.39
		0.79			8.87
		1.13			13.59
		1.49			18.30
		3.66			
		4.75	Helium*		
		7.46	(99.995%)	60-110	1.31
		9.01			3.45
					4.51
Helium					7.32
(99.995%)	105-150	0.93			14.08
		3.31			18.52
		4.72			
		6.34	Argon	60-110	
		10.7	(99.995%)	60-110	0.11
		12.81			0.29
		18.66			0.45
					0.46
Helium					
(99.995%)	145-200	1.35			
		5.17			
		8.80			
		13.70			
		17.74			

*Liquid nitrogen cooled zeolite trap used for helium test gas - all others, no trap.

TABLE II

SUMMARY OF EXPERIMENTAL PARAMETERS

Test Gas and Wavelength Range (nm)	UV Source	Detector	Wavelength Scan Rate nm/min	Slit Width entrance-exit μm	Path Length cm
Helium-99.995% 60-110	Helium Continuum P_{He} = 122 mm Hg Air-gap Spark-20 ma	1175 V 0.3 μA scale	10	50-10	61
Helium-99.995% 100-160	Argon Continuum P_{Ar} = 110 mm Hg Air-gap Spark-20 ma	1150 V 0.3 μA scale	10	50-10	61
Helium-99.995% 145-200	Xenon Continuum P_{Xe} = 110 mm Hg Air-gap Spark-20 ma	1175 V 0.3 μA scale	10	50-10	61
Helium-99.995% 220-300	Quartz-iodine, tungsten filament lamp - 8.3 amp	1175 V 0.3 μA scale	10	50-10	61
Helium-99.995% 60-110 (with cooled zeolite trap)	Helium Continuum P_{He} = 121 mm Hg Air-gap Spark-20 ma	1125 V 0.1 μA scale	10	50-10	61
Argon-99.995% 60-110	Helium Continuum P_{He} = 110 mm Hg Air-gap Spark-20 ma	1200 V 0.3 μA scale	10	50-10	61
UF_6/Argon 60-200	Helium Continuum P_{He} = 95 mm Hg Air-gap Spark-20 ma	1200 V 0.3 μA scale	25	50-10	1.91

TABLE III

UF_6 AND ARGON PRESSURES AND UF_6/Ar

PRESSURE RATIOS

USED FOR SPECTRAL ABSORPTION MEASUREMENTS

Series	P_A, mm Hg	P_{UF_6}, mm Hg	P_{UF_6}/P_{Ar}
A-1	31.5	0.62	1.97×10^{-2}
A-2		0.22	6.98×10^{-3}
A-3		1.72	5.46×10^{-2}
B-1	45.8	1.71	3.73×10^{-2}
B-2		0.48	1.05×10^{-2}

TABLE IV

ABSORPTION CROSS SECTIONS OF URANIUM HEXAFLUORIDE

Superscripts A and B and Subscripts 1, 2, and 3 Refer to Test Series Pressures Given in Table III.

λ nm	σ_1^A	σ_2^A	σ_3^A	σ_1^B	σ_2^B	(σ)
	← cm^2 →					
80.0	1.37-17	--	--	1.84-17	1.09-17	1.43-17
82.5	1.31-17	5.80-18	2.18-17	1.75-17	1.31-17	1.42-17
85.0	1.68-17	9.58-18	2.22-17	2.24-17	1.42-17	1.70-17
87.5	1.46-17	1.19-17	2.29-17	2.41-17	1.56-17	1.78-17
90.0	1.76-17	1.40-17	2.67-17	2.56-17	1.64-17	2.01-17
92.5	1.91-17	1.54-17	2.53-17	2.95-17	1.77-17	2.14-17
95.0	1.94-17	2.06-17	--	3.66-17	2.53-17	2.55-17
97.5	2.18-17	1.70-17	--	2.84-17	2.45-17	2.29-17
100.0	2.20-17	2.50-17	--	2.82-17	3.19-17	2.68-17
102.5	--	--	--	1.45-17	1.63-17	1.54-17
105.0	2.32-17	--	--	1.79-17	1.32-17	1.81-17
115.0	--	--	--	1.93-17	1.45-17	1.69-17
117.5	--	--	--	6.98-18	5.74-18	6.36-17
120.0	--	--	--	6.51-18	1.28-17	8.66-18

(σ) Denotes an average value

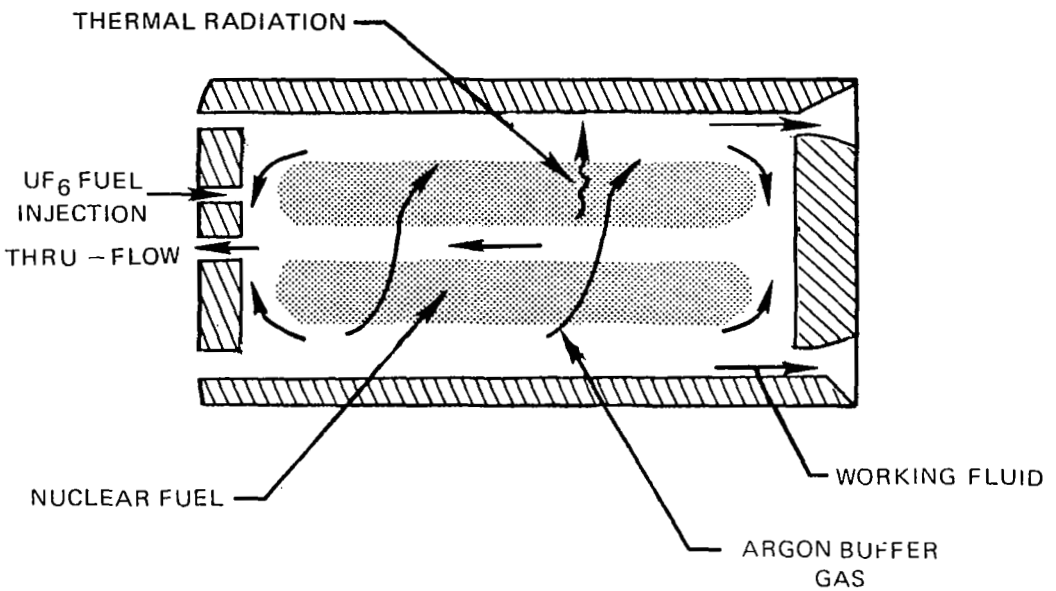

FIG. 1 SCHEMATIC OF A UNIT CAVITY OF A PLASMA CORE REACTOR

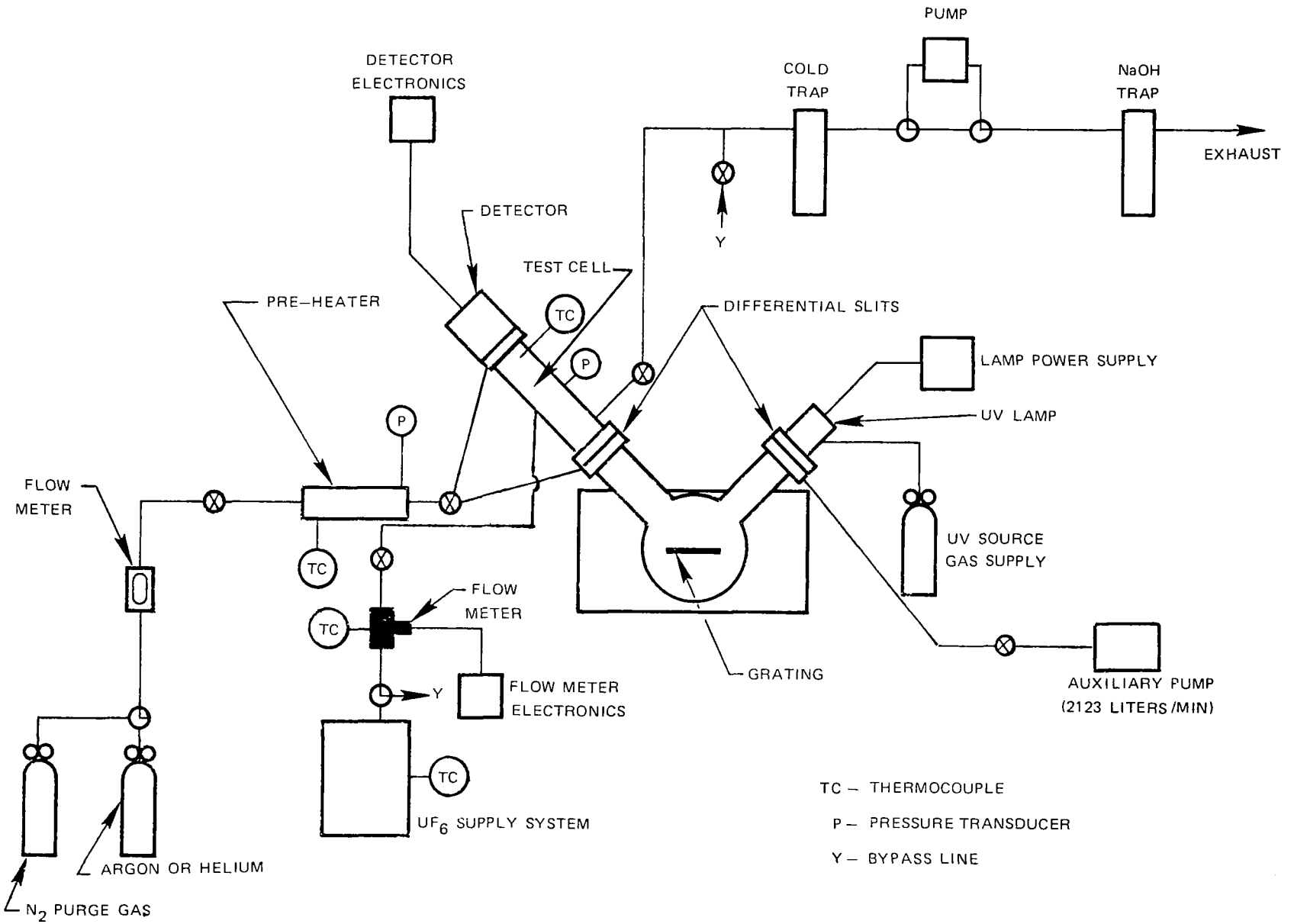

FIG. 2 VACUUM ULTRAVIOLET SPECTROMETER AND GAS TRANSFER SYSTEM

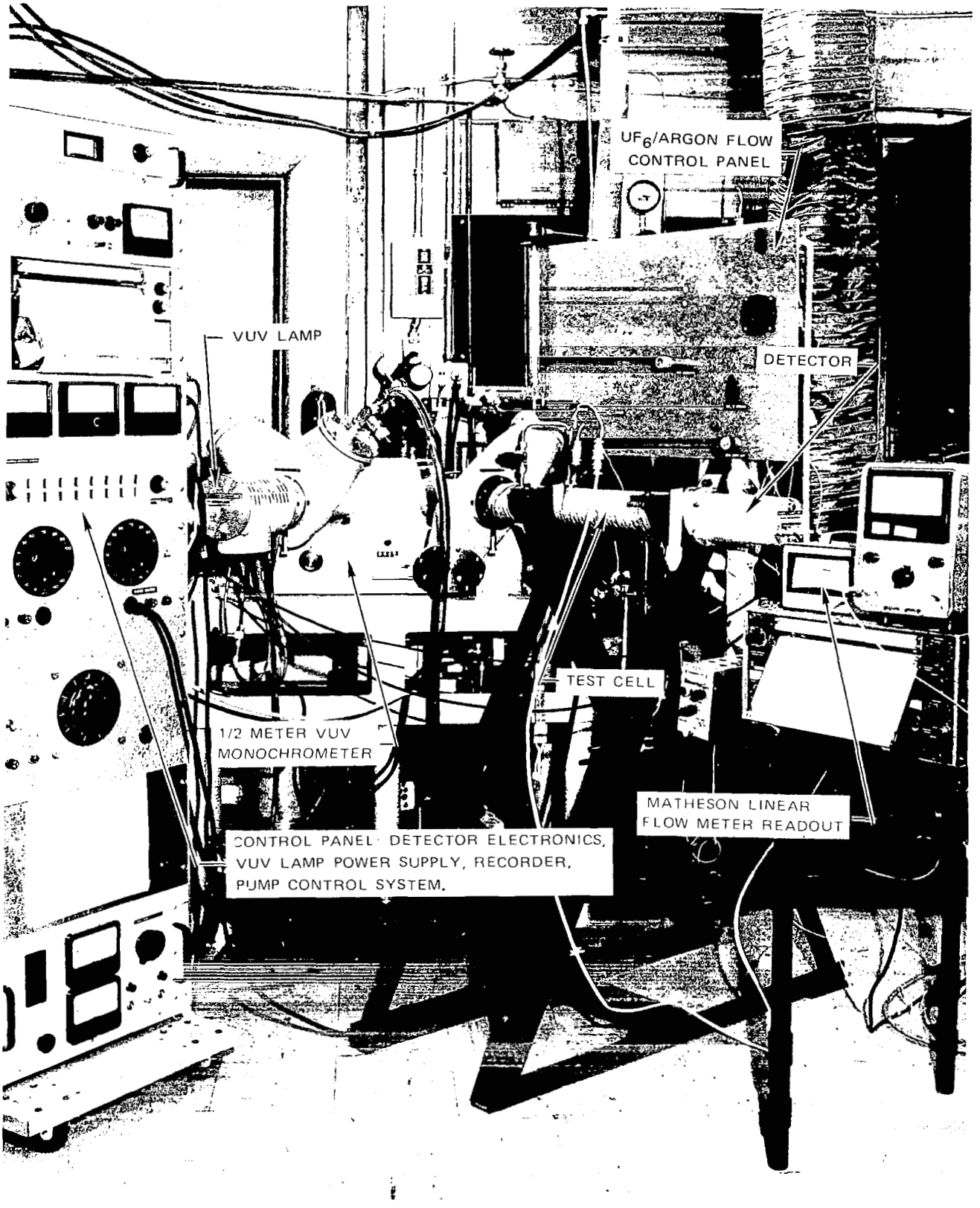

FIG. 3 VACUUM ULTRAVIOLET SPECTROMETER SYSTEM

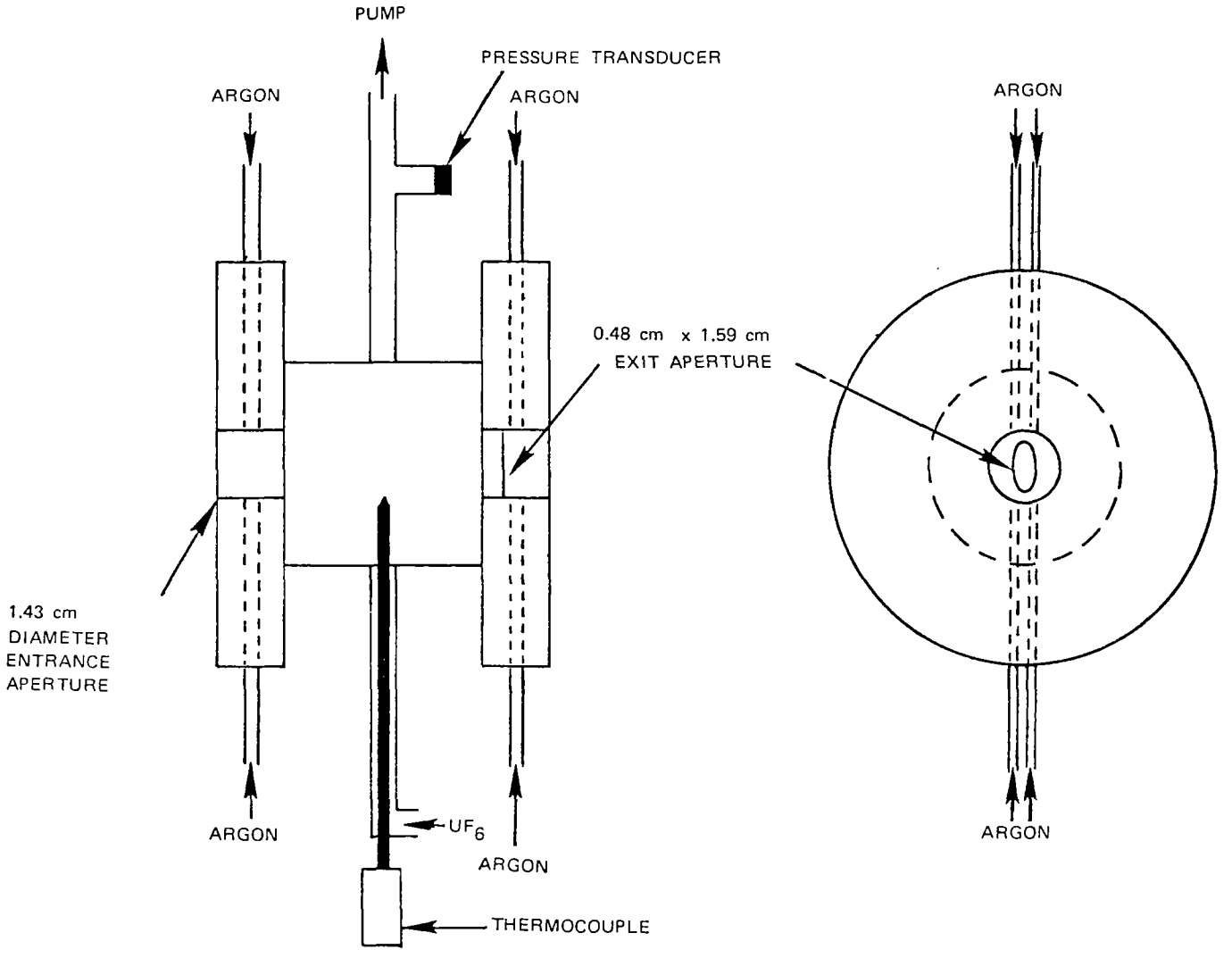

FIG. 4 SCHEMATIC OF UF_6/ARGON TEST CELL CONFIGURATION

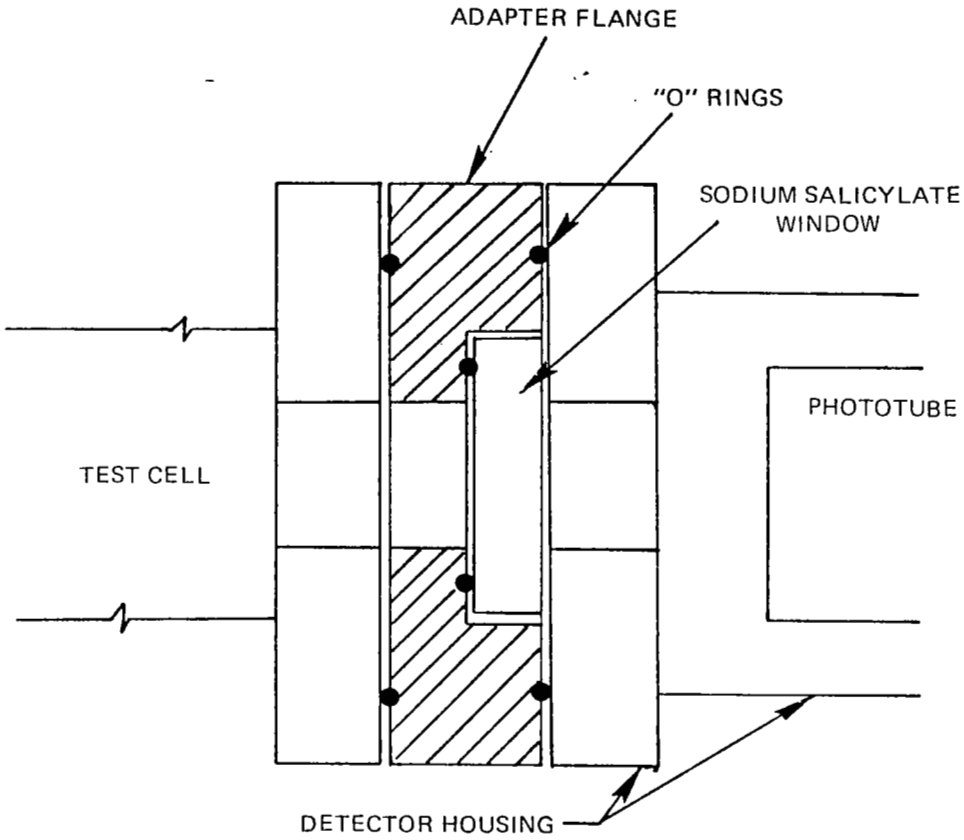

FIG. 5 SODIUM SALICYLATE WINDOW ADAPTER

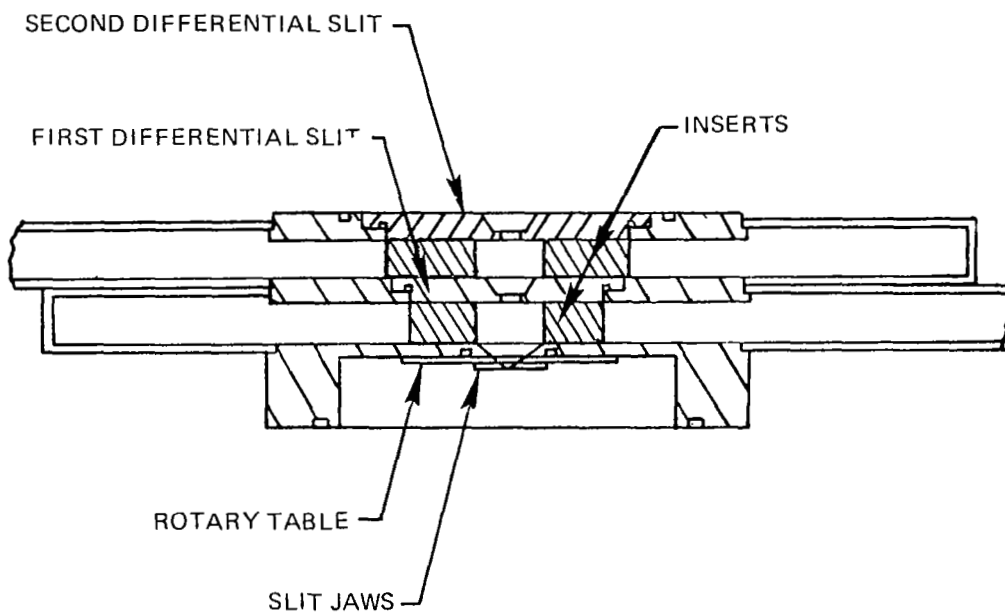

FIG. 6 DIFFERENTIAL SLIT ASSEMBLY MODIFICATION FOR HIGH PRESSURE OPERATION

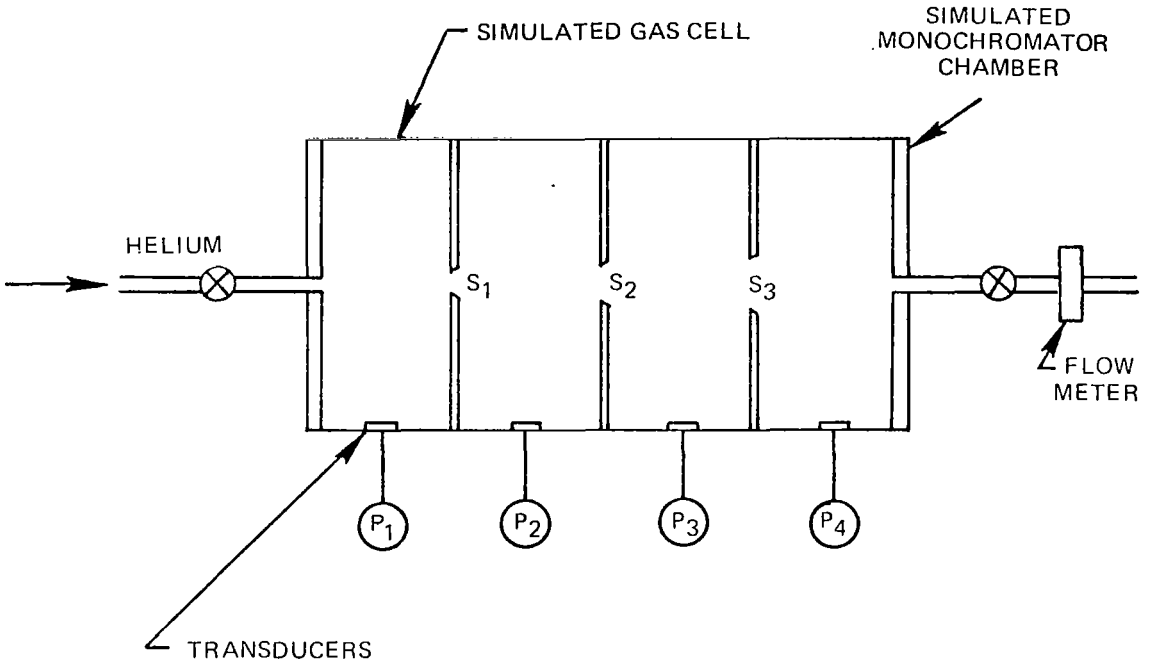

S_1 – VARIABLE WIDTH SLIT: 10, 50 or 100 μ x 1.25 cm

S_2 – FIRST DIFFERENTIAL SLIT: 0.183 cm x 0.498 cm

S_3 – SECOND DIFFERENTIAL SLIT: 0.351 cm x 0.584 cm

FIG. 7 DIFFERENTIAL SLIT ASSEMBLY FLOW AND PRESSURE TEST CONFIGURATION

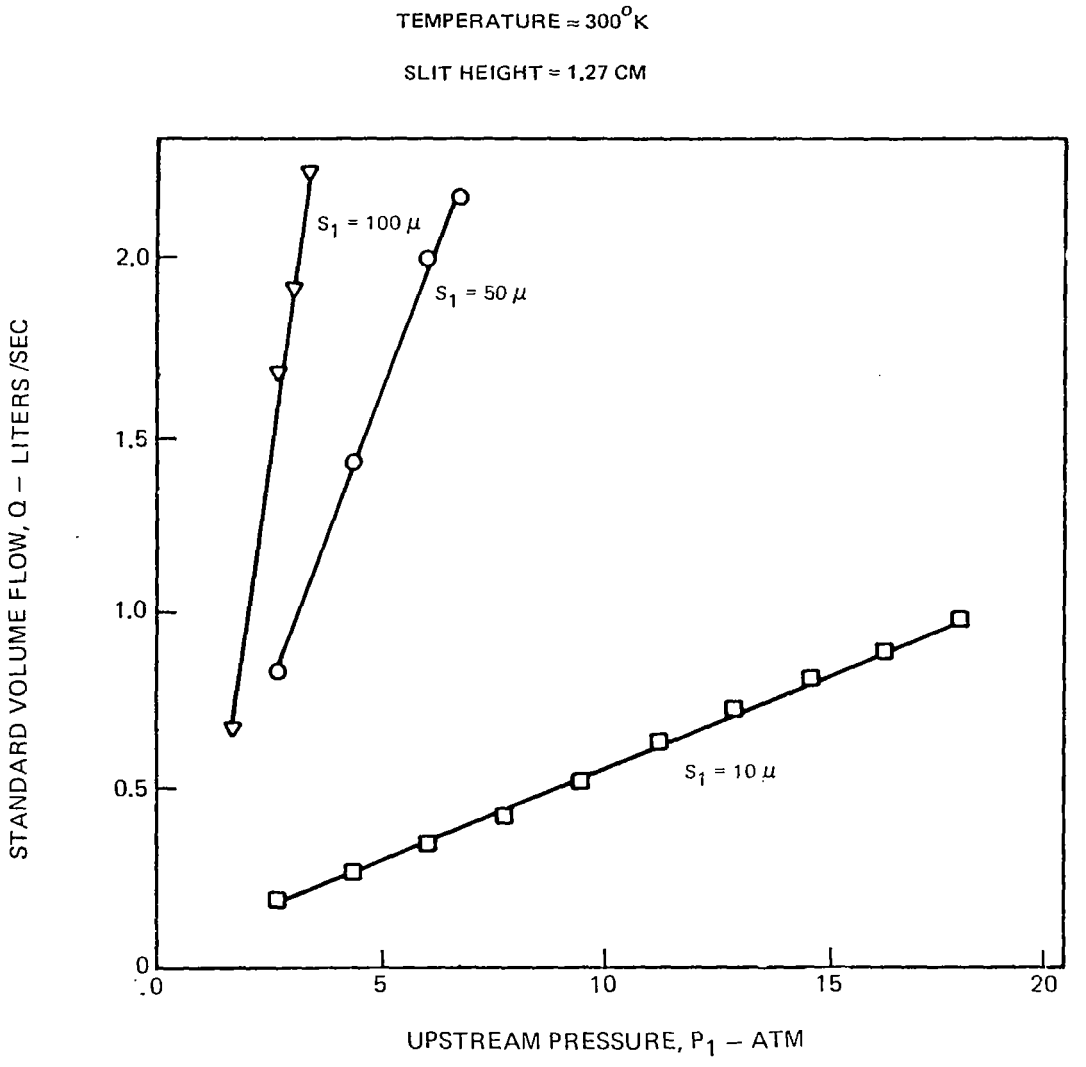

FIG. 8 COMPARISON OF HELIUM FLOW THROUGH VARIOUS SIZES OF DIFFERENTIAL SLITS, S_1, AS A FUNCTION OF PRESSURE, P_1

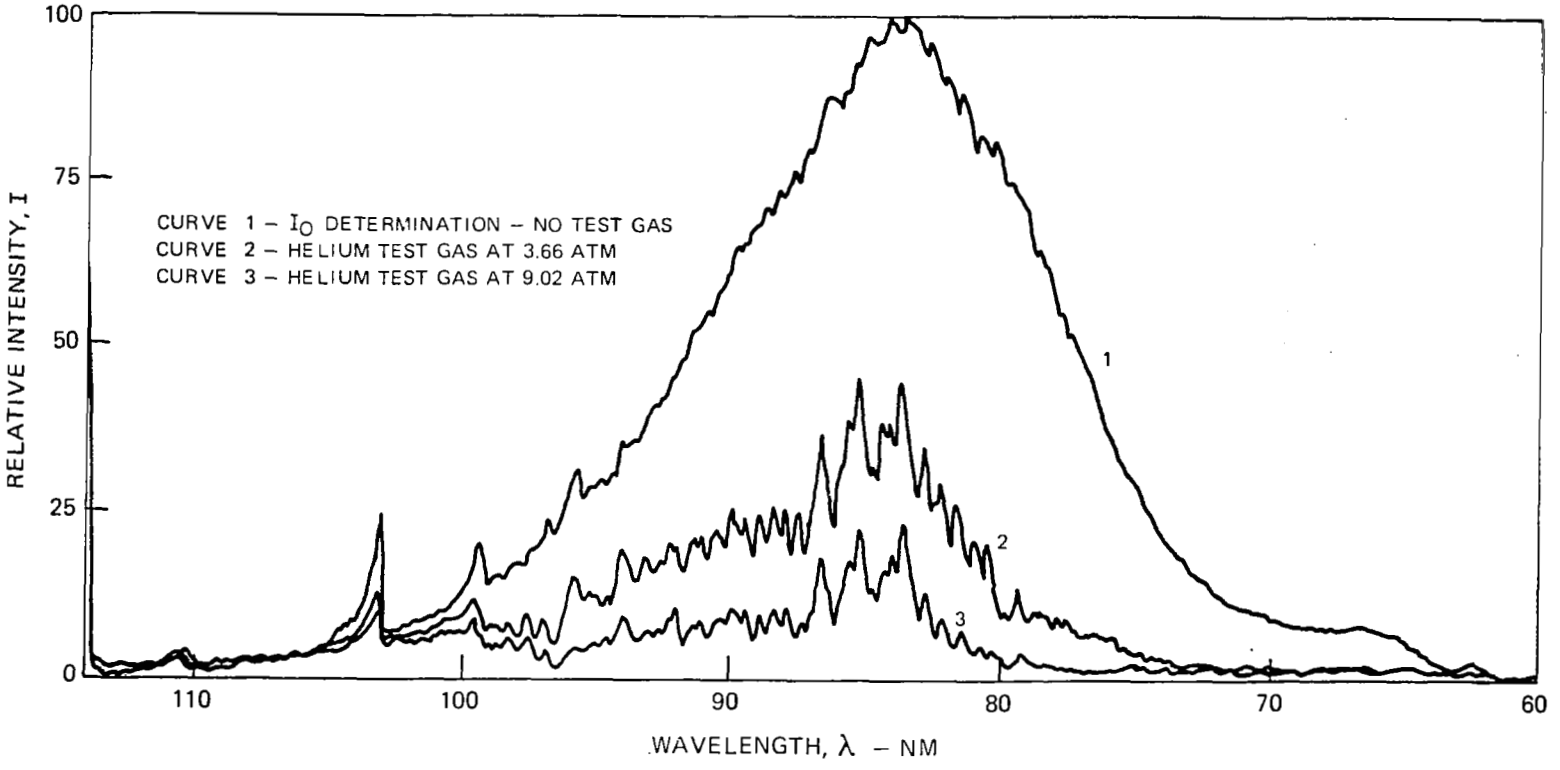

FIG. 9 RELATIVE SPECTRAL TRANSMISSION OF HELIUM BETWEEN 60 AND 110 NANOMETERS

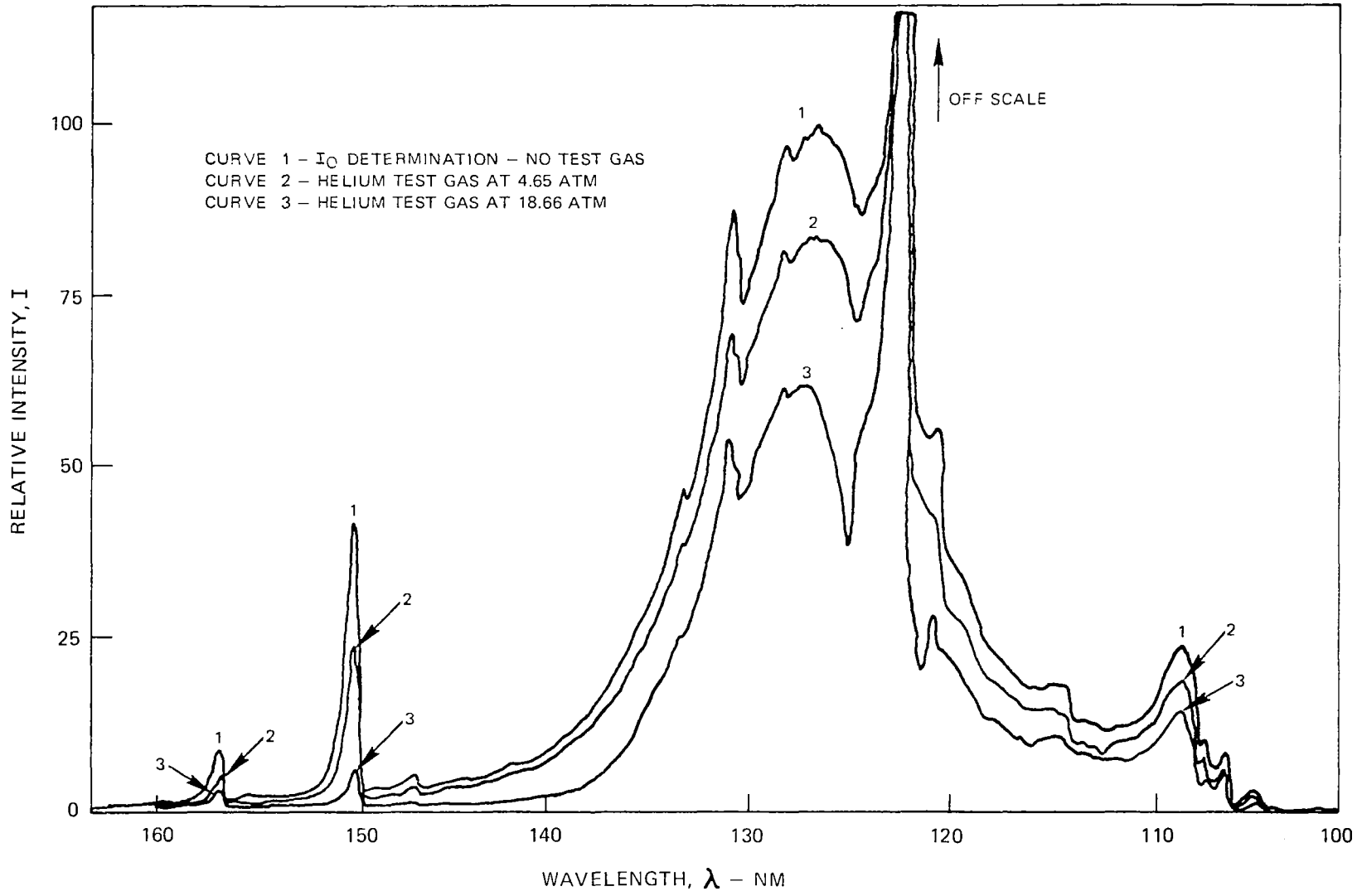

FIG. 10 RELATIVE SPECTRAL TRANSMISSION OF HELIUM BETWEEN 100 AND 160 NANOMETERS

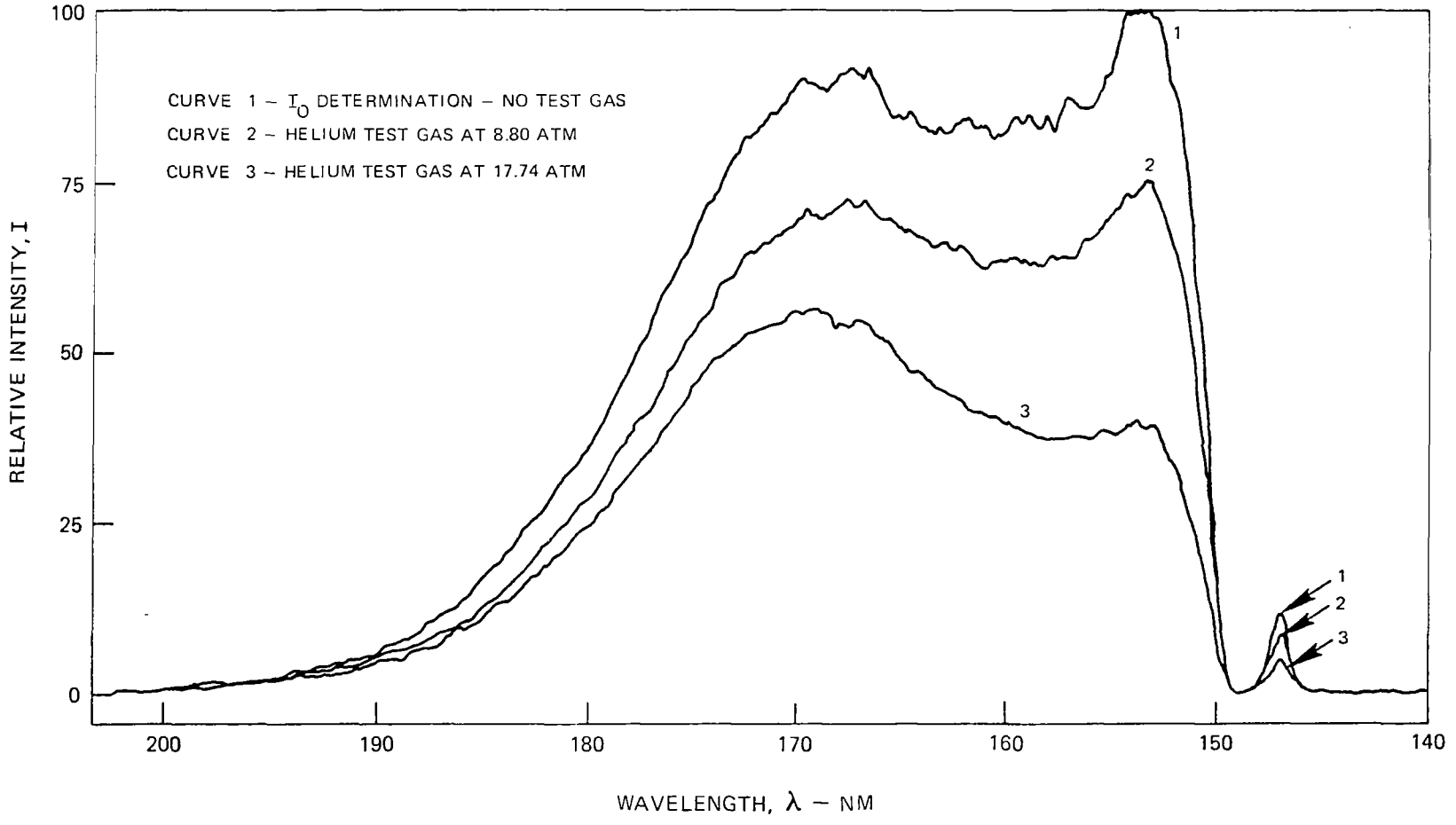

FIG. 11 RELATIVE SPECTRAL TRANSMISSION OF HELIUM BETWEEN 145 AND 200 NANOMETERS

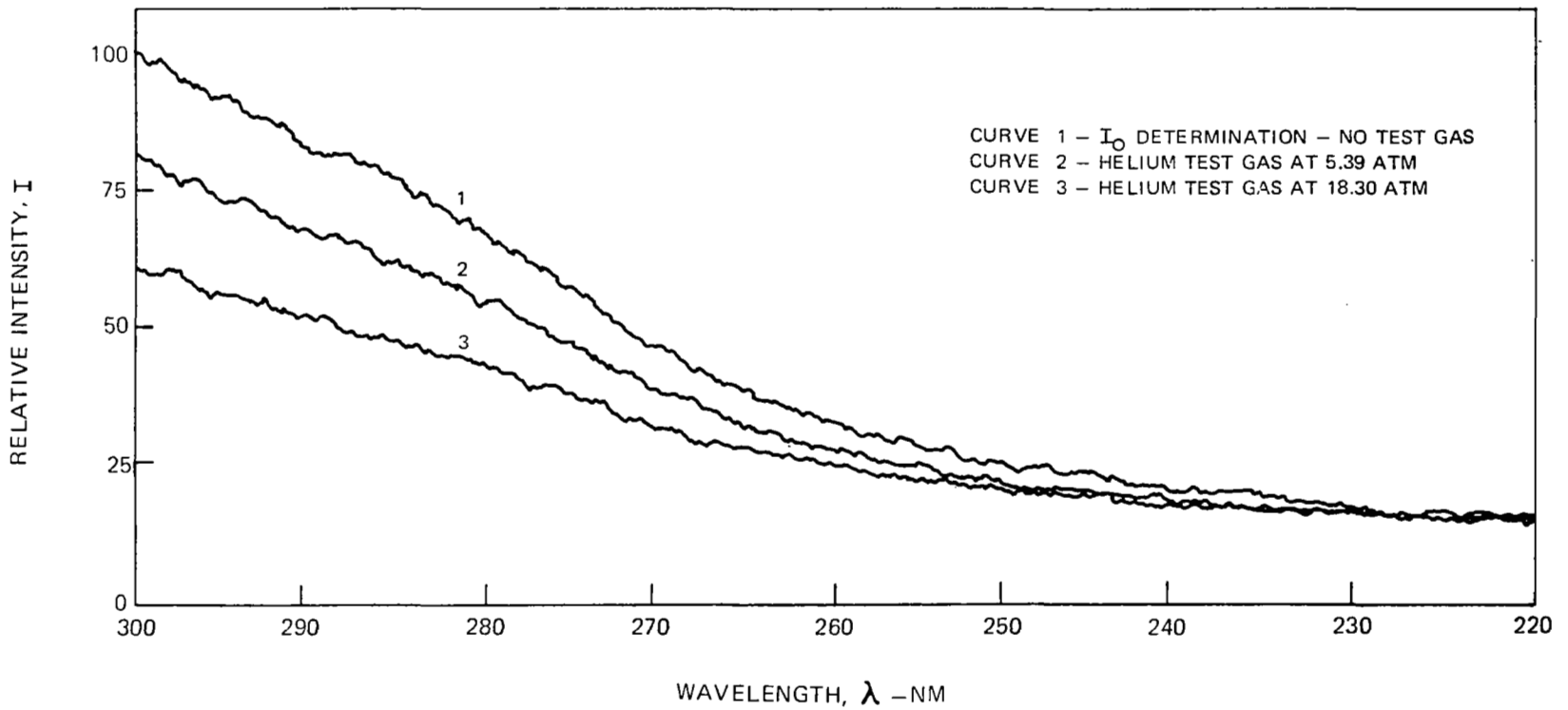

FIG. 12 RELATIVE SPECTRAL TRANSMISSION OF HELIUM BETWEEN 220 AND 300 NANOMETERS

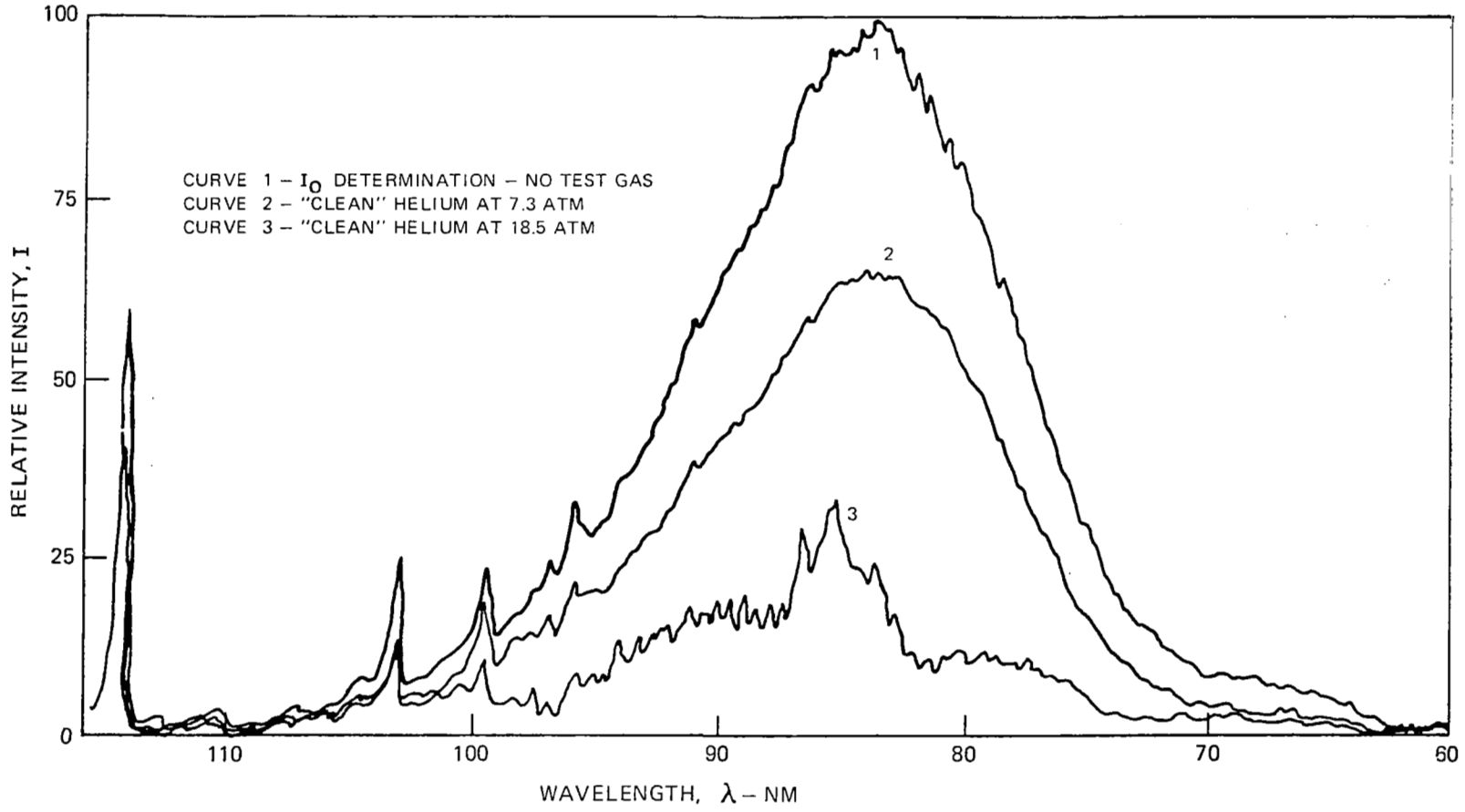

FIG. 13 RELATIVE SPECTRAL TRANSMISSION OF "CLEAN" HELIUM BETWEEN 60 AND 110 NANOMETERS

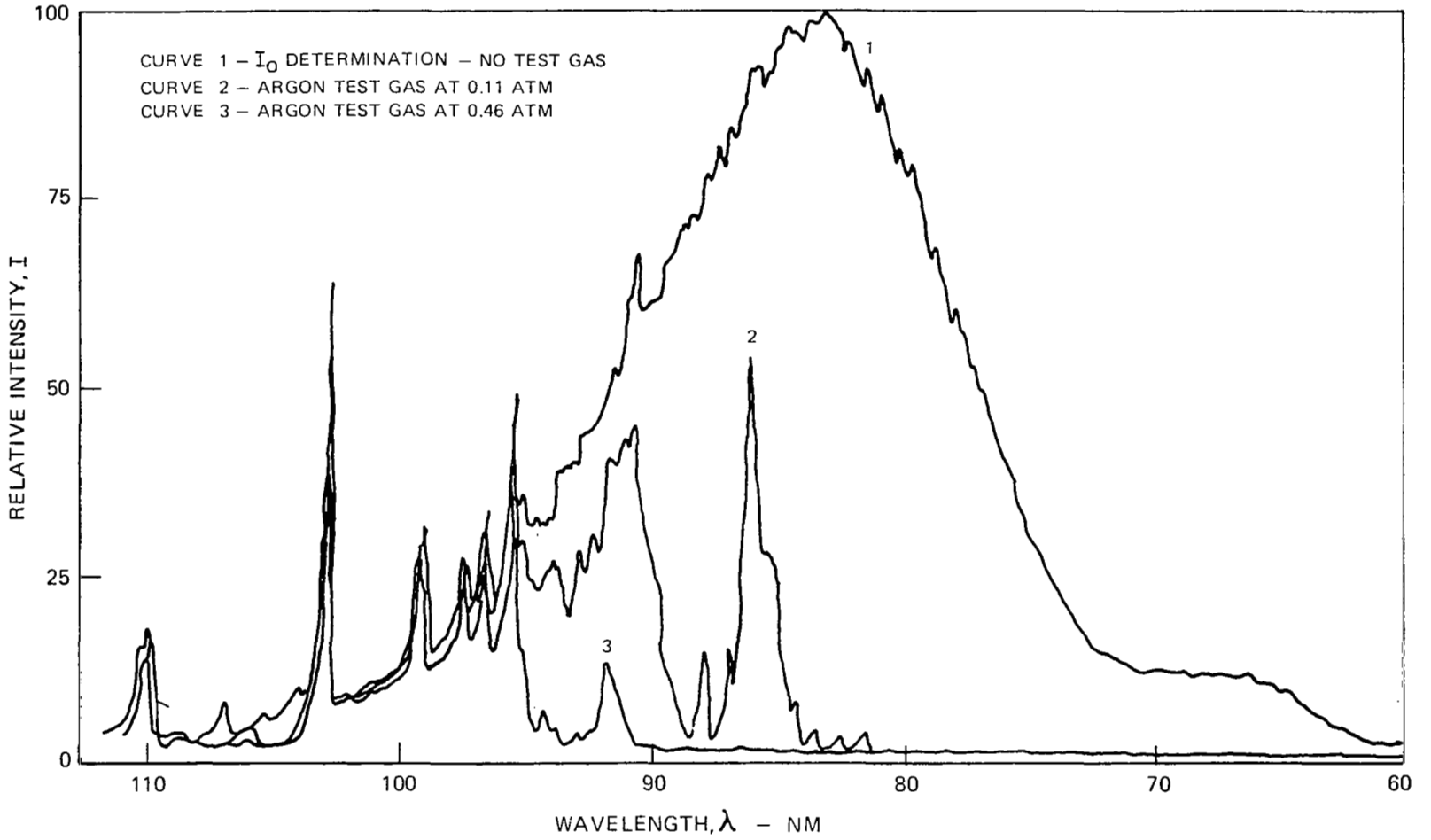

FIG. 14 RELATIVE SPECTRAL TRANSMISSION OF ARGON BETWEEN 60 AND 110 NANOMETERS

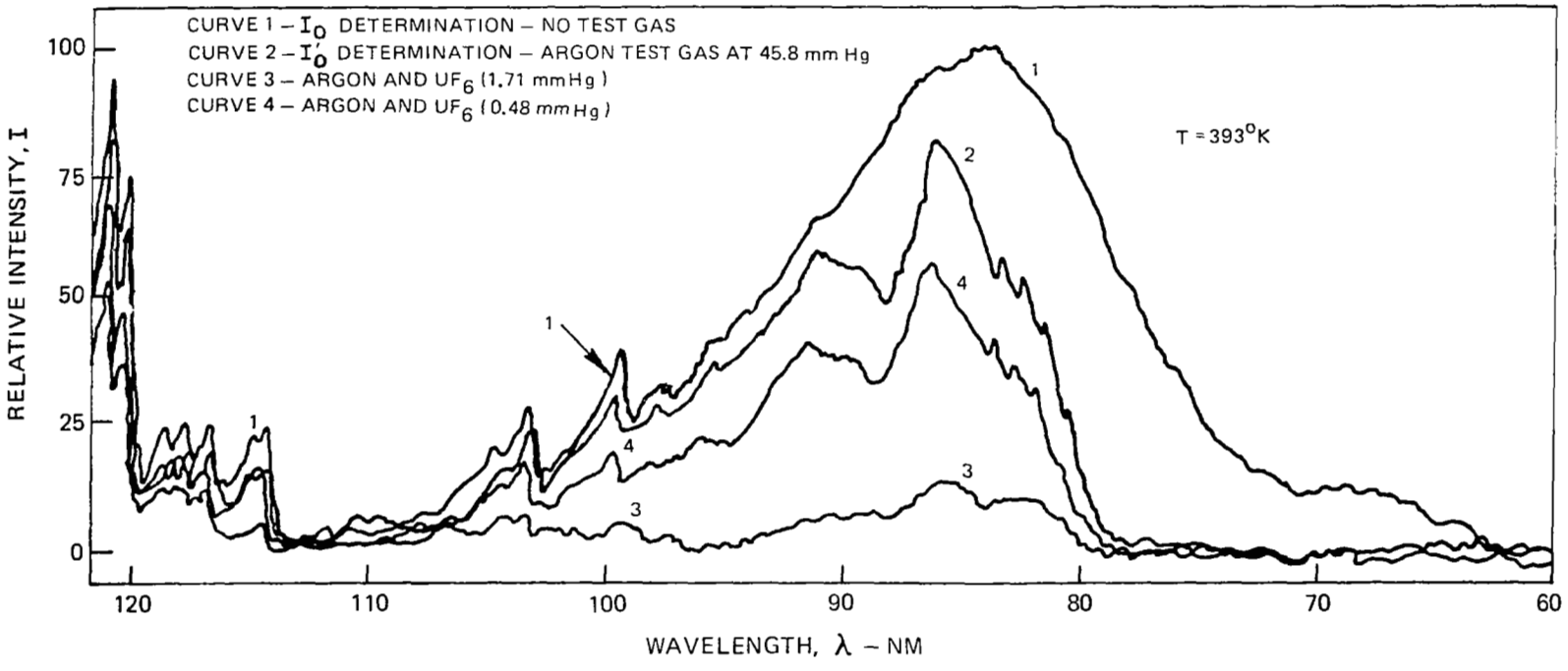

FIG. 15 RELATIVE SPECTRAL TRANSMISSION OF URANIUM HEXAFLUORIDE BETWEEN 60 AND 120 NANOMETERS

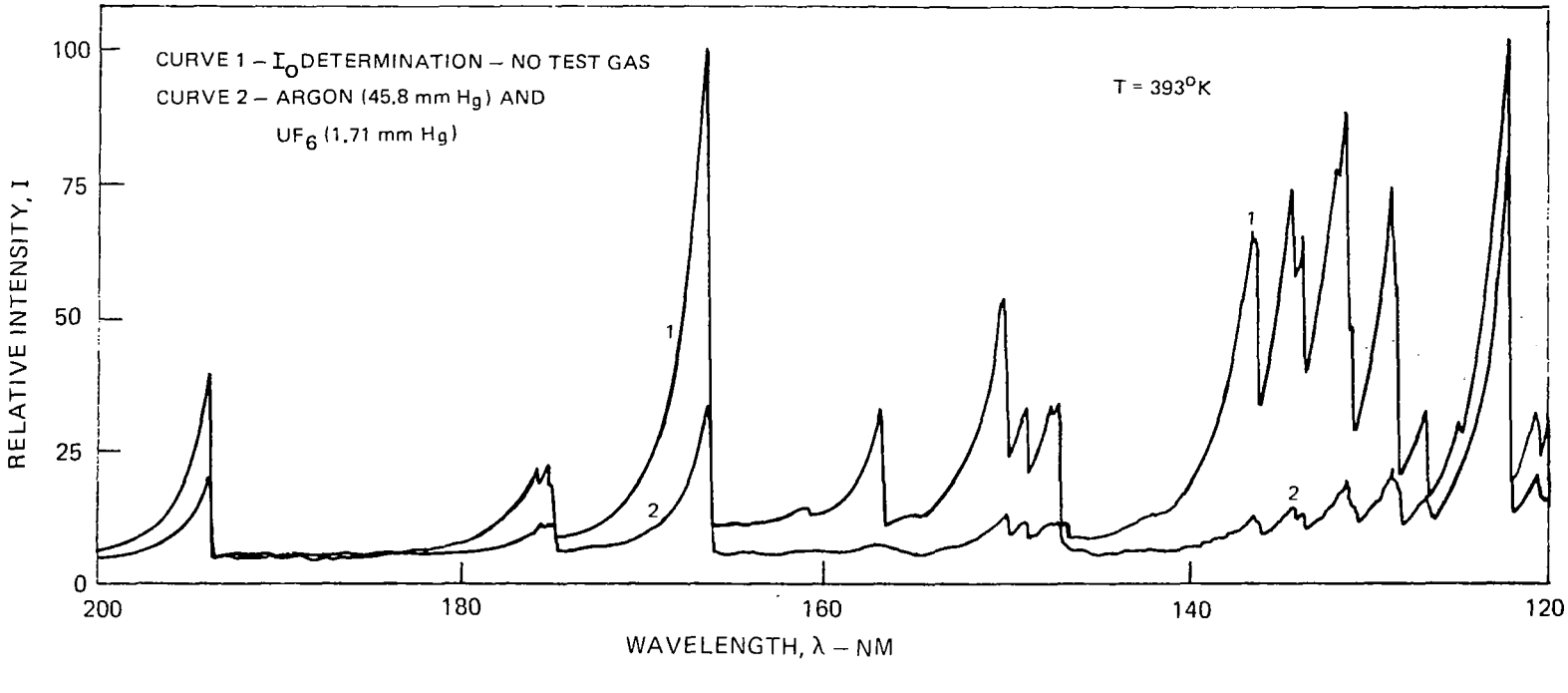

FIG. 16 RELATIVE SPECTRAL TRANSMISSION OF URANIUM HEXAFLUORIDE BETWEEN 120 AND 200 NANOMETERS

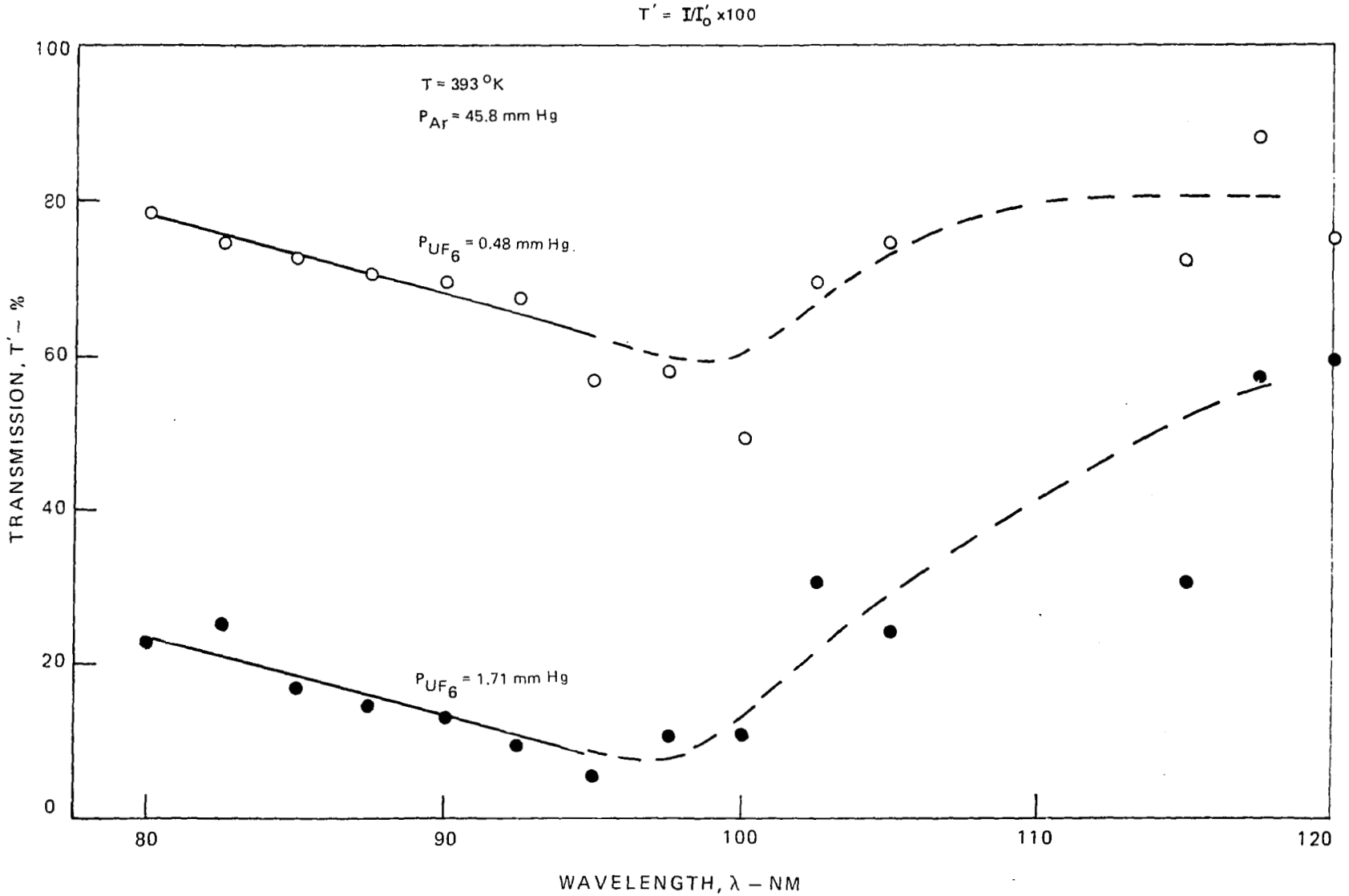

FIG. 17 SPECTRAL TRANSMISSION OF URANIUM HEXAFLUORIDE BETWEEN 80 AND 120 NANOMETERS

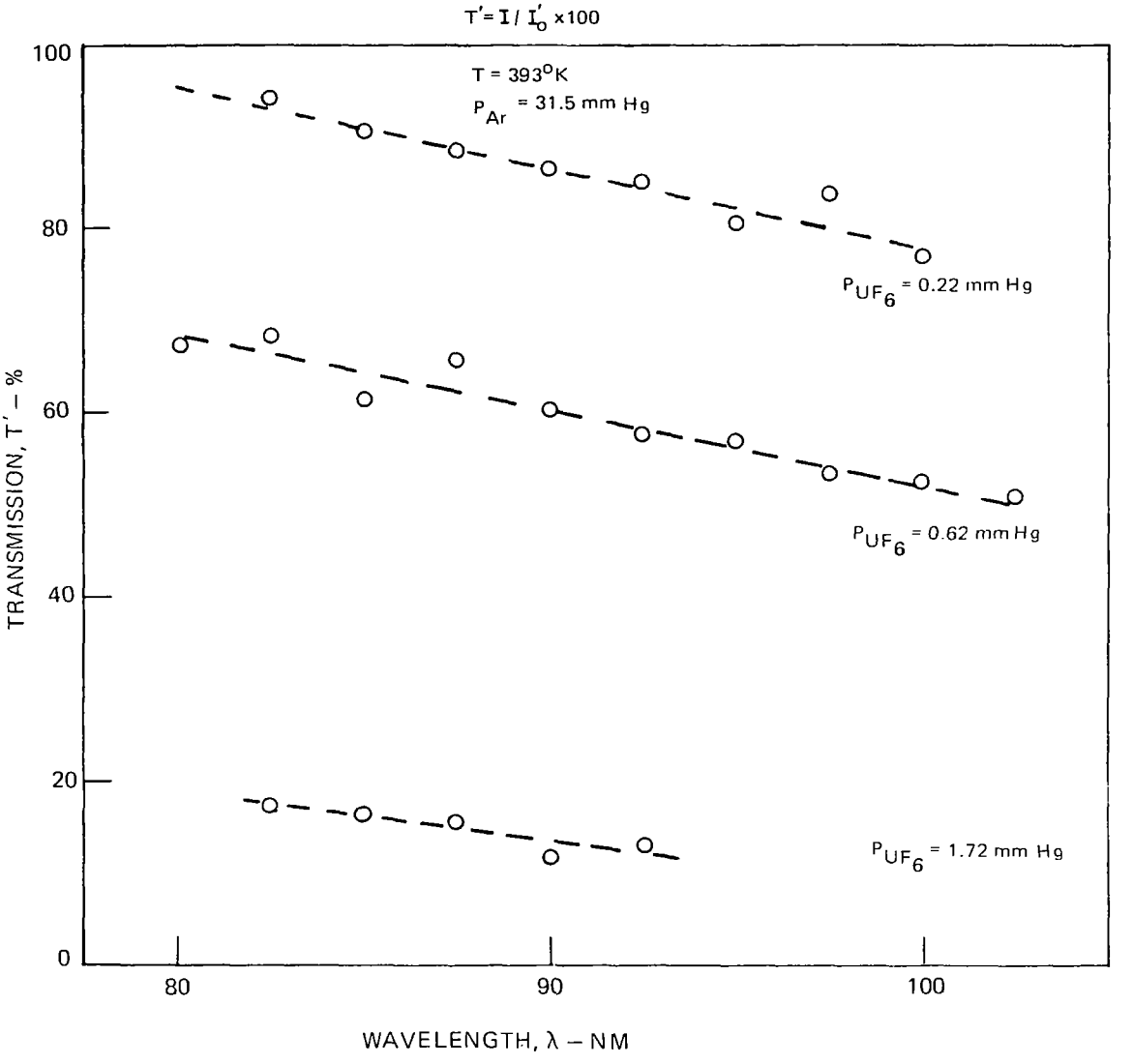

FIG. 18 SPECTRAL TRANSMISSION OF URANIUM HEXAFLUORIDE BETWEEN 80 AND 100 NANOMETERS

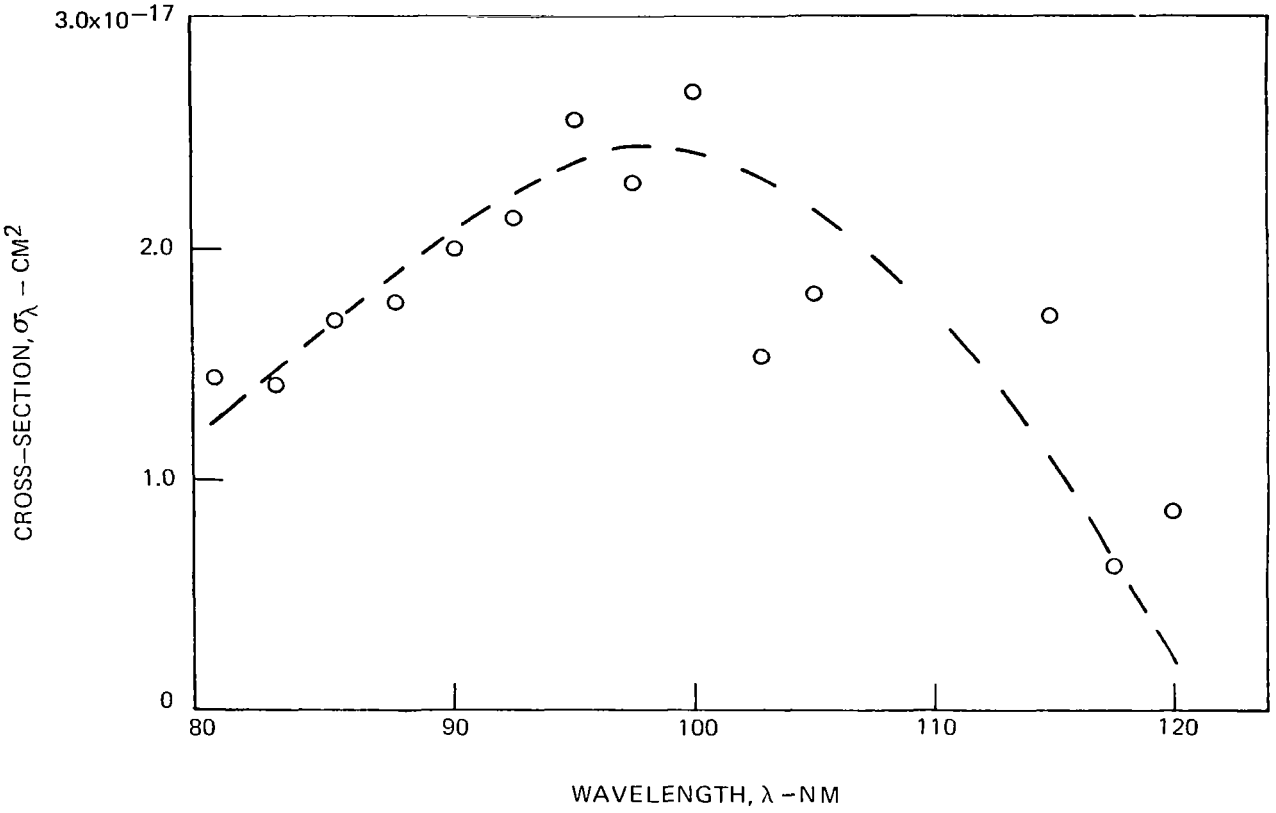

FIG. 19 ABSORPTION CROSS–SECTION OF URANIUM HEXAFLUORIDE BETWEEN 80 AND 120 NANOMETERS